

1
2
3
4
5
6
7
8
9
10
11
12
13
14
15
16
17
18
19
20
21
22
23
24
25
26
27

Impacts of future climate change on urban flood volumes in Hohhot City in Northern China: benefits of climate mitigation and adaptations

Qianqian Zhou^{1,2}, Guoyong Leng^{2,*}, Maoyi Huang³

¹School of Civil and Transportation Engineering, Guangdong University of Technology,
Waihuan Xi Road, Guangzhou 510006, China

²Joint Global Change Research Institute, Pacific Northwest National Laboratory, College Park
MD 20740, USA

³Earth System Analysis and Modeling Group, Pacific Northwest National Laboratory, Richland,
WA 99352, USA

*Corresponding author address: Guoyong Leng, Joint Global Change Research Institute, Pacific Northwest National Laboratory, College Park MD, 20740.

E-mail: guoyong.leng@pnnl.gov

28 **Abstract**

29 As China has become increasingly urbanised, flooding has become a regular occurrence in its
30 major cities. Assessing the effects of future climate change on urban flood volumes is crucial to
31 informing better management of such disasters given the severity of the devastating impacts of
32 flooding (e.g., the 2016 flooding across China). Although recent studies have investigated the
33 impacts of future climate change on urban flooding, the effects of both climate change mitigation
34 and adaptation have rarely been accounted for together in a consistent framework. In this study,
35 we assess the benefits of mitigating climate change by reducing greenhouse gas emissions and
36 locally adapting to climate change by modifying drainage systems to reduce urban flooding
37 under various climate change scenarios through a case study conducted in Northern China. The
38 urban drainage model—Storm Water Management Model—was used to simulate urban flood
39 volumes using current and two adapted drainage systems (i.e., pipe enlargement and low-impact
40 development), driven by bias-corrected meteorological forcing from five general circulation
41 models in the Coupled Model Intercomparison Project Phase 5 archive. Results indicate that
42 urban flood volume is projected to increase by 52% in 2020–2040 compared to the volume in
43 1971–2000 under the business-as-usual scenario (i.e., Representative Concentration Pathway
44 (RCP) 8.5). The magnitudes of urban flood volumes are found to increase nonlinearly with
45 changes in precipitation intensity. On average, the projected flood volume under RCP 2.6 is 13%
46 less than that under RCP 8.5, demonstrating the benefits of global-scale climate change
47 mitigation efforts in reducing local urban flood volumes. Comparison of reduced flood volumes
48 between climate change mitigation and local adaptation (by improving the drainage system)
49 scenarios suggests that local adaptation is more effective than climate change mitigation in
50 reducing future flood volumes. This has broad implications for the research community relative

51 to drainage system design and modelling in a changing environment. This study highlights the
52 importance of accounting for local adaptation when coping with future urban floods.

53

54 **Keywords:** Climate change, urban floods, mitigation, adaptation, drainage systems

55

56 1. Introduction

57 Floods are one of the most hazardous and frequent disasters in urban areas and can cause
58 enormous impacts on the economy, environment, city infrastructure, and human society (Chang
59 et al., 2013; Ashley et al., 2007; Zhou et al., 2012). Urban drainage systems have been
60 constructed to provide carrying and conveyance capacities at a desired frequency to prevent
61 urban flooding. However, the design of drainage systems is often based on historical
62 precipitation statistics for a certain period of time, without considering the potential changes in
63 precipitation extremes for the designed return periods (Yazdanfar and Sharma, 2015; Peng et al.,
64 2015; Zahmatkesh et al., 2015). It is likely that drainage systems would be overwhelmed by
65 additional runoff induced by climate change, which may lead to increased flood frequency and
66 magnitude, disruption of transportation systems, and increased human health risk (Chang et al.,
67 2013; Abdellatif et al., 2015). For example, Arnbjerg-Nielsen (2012) reported that the design
68 intensities in Denmark are projected to increase by 10-50% for return periods ranging from 2 to
69 100 years. Therefore, it is important to investigate the performance of drainage systems in a
70 changing environment and to assess the potential urban flooding under various scenarios to
71 achieve better adaptations (Mishra, 2015; Karamouz et al., 2013; Yazdanfar and Sharma, 2015;
72 Notaro et al., 2015).

73

74 Impacts of climate change on extreme precipitation and urban flooding have been well
75 documented in a number of case studies. For example, Ashley et al. (2005) showed that flooding
76 risks (i.e., occurrence of pluvial floods) in four UK catchments may increase by almost 30 times
77 by 2080s compared to current conditions around the year 2000, and effective adaptation
78 measures are required to cope with the increasing risks in the UK. Larsen et al. (2009) estimated
79 that future extreme one-hour precipitation will increase by 20%~60% throughout Europe by
80 2071–2100 relative to 1961–1990. Willems (2013) found that in Belgium the current design
81 storm intensity for the 10-year return period is projected to increase by 50% by the end of this
82 century. Several studies have also investigated the role of climate change mitigation or
83 adaptation in reducing urban flood damages and risks under climate change scenarios (Alfieri et
84 al., 2016; Arnbjerg-Nielsen et al., 2015; Moore et al., 2016; Poussin et al., 2012). The
85 relationship between changes in precipitation intensity and flood volume has also been well
86 explored to provide additional insights into drainage design strategies (Olsson et al., 2009;
87 Willems et al., 2012; Zahmatkesh et al., 2015). However, previous studies on the effects of
88 climate change mitigation and adaptation are typically conducted separately, and it is unclear
89 which strategy is more effective in reducing urban floods. This study aims to advance our
90 understanding on urban floods within the context of change climate, through investigating the
91 benefits of climate change mitigation (by reducing greenhouse gas emissions [GHG]) and local
92 adaptation (by improving drainage systems) in reducing future urban flood volumes in a
93 consistent framework.

94

95 As China has become increasingly urbanised, flooding has become a regular occurrence in its
96 cities; 62% of Chinese cities surveyed experienced floods and direct economic losses of up to

97 \$100 billion between 2011 and 2014 (China Statistical Yearbook 2015). The 2016 flooding
98 affected more than 60 million people—more than 200 people were killed and \$22 billion in
99 losses were suffered across China. Hence, assessing future changes in urban flooding is very
100 important for managing urban floods by designing new and re-designing existing urban
101 infrastructures to be resilient in response to the impacts of future climate change. While urban
102 floods are speculated to increase in the future (Yang 2000; Ding et al., 2006), their magnitudes
103 are hard to assess because of uncertainties associated with future climate change scenarios, as
104 well as the under-representation of plausible climate change mitigation and adaptation strategies
105 in the models.

106

107 In this study, we chose a drainage system in a typical city in Northern China to illustrate the role
108 of climate change mitigation and local adaptation in coping with future urban flood volumes.
109 Such an investigation of the performance of the present-day drainage system also has important
110 implications for local governments responsible for managing urban flood disasters in the study
111 region. Specifically, we first quantified the effects of future climate change on urban flood
112 volumes as a result of extreme precipitation events for various return periods using the present-
113 day drainage system. We then designed two plausible adaptation strategies for the study region
114 and investigated how much urban flood volume can be reduced with the adapted systems by
115 2020s. We also compared the benefits of global-scale climate change mitigation and local
116 adaptation in reducing urban flood volumes to advance our understanding of the effective
117 measures for coping with future urban floods.

118

119 2. Materials and Methods

120 a. Study region

121 The study region (Hohhot City) is located in the south-central portion of Inner Mongolia, China.
122 It lies between the Great Blue Mountains to the north and the Hetao Plateau to the south, which
123 has a north-to-south topographic gradient. The region is in a cold semi-arid climate zone,
124 characterised by cold and dry winters and hot and humid summers. The regional annual mean
125 precipitation is approximately 396 mm with large intra-seasonal variations. Most rain storms fall
126 between June and August, a period that accounts for more than 65% of the annual precipitation.
127 The drainage area in year 2010 was about 210.72 km² and it served a residential population of
128 1.793 million (Figure 1a). The land use types in the region can be classified into five categories:
129 agricultural land (8%), residential areas (38%), industrial land (13%), green spaces (7%), and
130 other facilities (34%, including municipal squares, commercial districts, institutions). According
131 to local water authorities, the major soil type of the area is a mixture of loam and clay.

132
133 The current drainage system can be divided into three large sub-basins (Figure 1c) and 326 sub-
134 catchments with a total pipeline length of 249.36 km. The drainage network has a higher pipeline
135 cover rate in the central part, but a rather low design standard for extreme rainfall events with a
136 return period of less than 1 year. Historical records of stormwater drainage and flood damage
137 indicate that the region has experienced an increase in flood frequency and magnitude within the
138 context of climate change and urbanisation (Zhou et al., 2016). During the major flood event on
139 11 July 2016, the city, especially the western portion of the watershed, was hit by an extreme
140 rainfall event that featured more than 100 mm of rain in 3 hours. The flood event led to the
141 cancellation of at least 8 flights and 17 trains, and delays of several transportation systems. In

142 particular, in the central area, the flood event caused severe traffic jams on major streets and
143 resulted in a number of flooded residential buildings. A new drainage system is therefore
144 required to cope with increasing urban flood volumes and frequencies in the future. The planned
145 drainage area for 2020s is about 307.83 km², which is 50% larger than the current drainage area
146 (Zhou et al., 2016). The land use categories and distribution are shown in Figure 1b.

147

148 b. Climate change scenarios

149 Climate projections by five general circulation models (GCMs) from Phase 5 of the Coupled
150 Model Intercomparison Project (CMIP5) archive were obtained from the Inter-Sectoral Impact
151 Model Intercomparison Project (ISI-MIP) (Warszawski et al., 2014). The CMIP5 climate
152 projections were bias-corrected against observed climate for the overlapping period 1950–2000
153 using a quantile mapping method (Piani et al., 2010; Hempel et al., 2013). The bias-corrected
154 CMIP5 climate projections represent a complete climate change picture that includes both the
155 mean property and variation of future climate. Several studies have demonstrated the value of the
156 bias-corrected climate projections in quantifying climate change impacts on global and regional
157 hydrology (e.g., Piontek et al., 2014; Elliott et al., 2014; Haddeland et al., 2014; Leng et al.,
158 2015a,b). In this study, we used the bias-corrected climate from five GCMs (HadGEM2-ES,
159 GFDL-ESM2M, IPSLCM5A-LR, MIROC-ESM-CHEM, and NorESM1-M) under two
160 Representative Concentration Pathways (RCPs) (i.e., RCP 2.6 and RCP 8.5). The projected
161 urban flood volumes under the business-as-usual scenario RCP 8.5 are compared with those
162 under the climate change mitigation scenario RCP 2.6 to explore the benefits of climate change
163 mitigation in reducing regional urban flood volumes. The possible land-surface-atmosphere
164 interactions that would indirectly affect rainfall and flooding are not considered in this study.

165

166 c. Urban drainage modelling

167 The Storm Water Management Model (SWMM 5.1) developed by the U.S. Environmental
168 Protection Administration is a widely used urban stormwater model that can simulate rainfall-
169 runoff routing and pipe dynamics under single or continuous events (Rossman and Huber, 2016).
170 SWMM can be used to evaluate the variation in hydrological and hydraulic processes and the
171 performance of drainage systems under specific mitigation and adaptation scenarios in the
172 context of global warming. The hydrological component requires inputs of precipitation and
173 subcatchment properties including drainage area, subcatchment width, and imperviousness. The
174 pipe network requires inputs from manholes, pipelines, outfalls, and connections to sub-
175 catchments (Zahmatkesh et al., 2015; Chang et al., 2013). Basic flow-routing models include
176 steady flow, kinematic, and dynamic wave methods. Infiltration can be described by the Horton,
177 Green-Ampt, or Curve Number (SCS-CN) methods. The dynamics of pipe flow are calculated
178 based on the continuity equation and Saint-Venant equations (Rossman and Huber, 2016).
179 Overflow occurs once the surface runoff exceeds the pipe capacity and is expressed as the value
180 of total flood volume (TFV) at each overloaded manhole; i.e., the excess water from manholes
181 after completely filling the pipe system without taking into account the outlet discharges. Other
182 types of model outputs include catchment peak flows, maximum flow rates of pipelines, and
183 flooded hours of manholes. It should be noted that SWMM is not capable of simulating surface
184 inundation dynamics and cannot provide accurate estimation of the inundated zones and depths.
185 The TFV value is thus used to approximately reflect the flood condition and drainage system
186 overloading status. Nevertheless, surface inundation models (e.g., Apel et al., 2009; Horritt and
187 Bates, 2002; Vojinovic and Tutulic, 2009) are applicable if more accurate information about

188 overland flow characteristics is available. In this study, the kinematic wave routing and the
189 Horton infiltration model are used for model simulations. The infiltration capacity parameters for
190 the category of "Dry loam soils with little or no vegetation" are used in the hydrological model to
191 be consistent with the local soil type (Akan, 1993; Rossman and Huber, 2016) (Supplementary
192 Materials, ST1).

193
194 Rainfall inputs are calculated based on the regional storm intensity formula (SIF) using historical
195 climatic statistics (Zhang and Guan, 2012) (Supplementary Materials, Equation 1-4). In this
196 study, we considered 10 return periods, i.e., the 1-, 2-, 3-, 10-, 20-, 50-, 100-, 200-, 500-, and
197 1000-year events. A 4-hour rainfall time series was generated for each return period at 10-minute
198 intervals. The duration of design rainfalls (i.e., 4-hour rainfall) is selected based on the time of
199 concentration (ToC) of the watershed in the study region, according to the design principles as
200 outlined in Butler and Davies (2010) and Chow et al. (2013). We assumed that the SIF was
201 constant without considering the non-stationary features in a changing climate. That is, the
202 Intensity-Duration-Frequency (IDF) relationships for estimating design rainfall hydrographs
203 were assumed to remain stable in the future and only changes in the daily mean intensity were
204 considered because of the limited data availability in future sub-hourly climate projections from
205 which to derive the parameters.

206
207 As for future climate, the projected changes (i.e., change factors) in precipitation intensity at
208 various return periods were calculated for each GCM-RCP combination (Table 1). Specifically,
209 for each year, the annual maximum daily precipitation was determined for both historical and
210 future periods. The generalised extreme value (GEV) distribution was then fitted separately to

211 the two sets of daily values (Coles 2001; Katz et al. 2002). Kolmogorov–Smirnov and
212 Anderson–Darling statistics show that the hypothesis regarding the extreme value distribution is
213 not rejected. That is, the fitted distribution could be well used to describe the extreme
214 precipitation distribution in the study region. The value corresponding to each return period was
215 estimated based on the GEV distribution and the changes between future and historical periods
216 were calculated as the change factors. The derived change factor for each return period was then
217 multiplied by the historical design CDS rainfall time series to derive future climate scenarios.
218 We acknowledge that the estimation of changes in extreme precipitation events involves
219 inevitable uncertainties and therefore caution should be exercised when interpreting the relevant
220 results.

221

222 d. Flood volume assessment

223 The total flood volume (TFV) values of given rainfall events were simulated by the SWMM. A
224 log-linear relationship is assumed to characterize the changes in flood volume with the increase
225 in precipitation intensity as indicated by return periods (Figure 2a) following Zhou et al. (2012)
226 and Olsen et al. (2015). Generally, more TFV (i.e., system overloading) is expected with increase
227 in rainfall intensity. In Figure 2b, the TFVs were linked to their specific occurrence probabilities.
228 The total grey area under the curve denotes the TFVs integrated across various return periods
229 and represents the total expected TFVs per year. The contribution of an individual flood event to
230 total average TFVs is dependent not only on the flood volume, but also its corresponding
231 probability of occurrence. Intensified precipitation is expected to increase the magnitude of
232 system overflow, resulting in an upward trend in the TFV-return period relationship and
233 increased total TFVs.

234

235 e. Design of adaptation scenarios

236 In this study, two adaptation scenarios were designed to explore the role of adaptation in
237 reducing urban flood volume within the context of climate change by 2020s. The first scenario
238 was designed to update the drainage system as planned by local water authorities to cope with
239 the standard 3-year design event. It involved two main improvements of the current drainage
240 system—enhancing the pipeline diameter and expanding the pipe network. The design was
241 implemented in the SWMM model as shown in Figure 1c. The number of pipelines of the
242 present-day and adapted systems was 323 and 488, with a total pipe length of 251.6 km and
243 375.4 km, respectively. In the adapted scenarios, the mean pipeline diameter was about 1.73 m,
244 which increased by 53% compared to that of the present-day system.

245

246 The second adaptation scenario was designed to increase the permeable surfaces (e.g., green
247 spaces) and reduce the regional imperviousness in the study region on the basis of pipe capacity
248 enhancement. This scenario is referred to as the Low Impact Development (LID) scenario, and it
249 was used to explore the effectiveness of urban green measures, such as the use of permeable
250 pavements, infiltration trenches, and green roofs. Changes in land imperviousness in LID
251 scenario have direct impacts on the performance of drainage system in managing surface runoff.
252 Due to a lack of detailed information about the permeable soil and coverage rates in the study
253 region, the effects of these specific measures cannot be modelled individually. Here, we used a
254 simplified approach by altering the subcatchment imperviousness to reflect the combined effects
255 of infiltration-related measures. We derived such information by calculating the difference in
256 land use type and imperviousness between the current and planned city maps using a

257 geographical information system (GIS). Figure 1d shows the difference in weighted mean
258 imperviousness ($WMI = \sum_i(IF_i \times A_i) / \sum_i A_i$, Where IF_i and A_i is the impervious factor and area
259 for land use type i , respectively.) for each subcatchment in the current and planned maps, using
260 the commonly applied impervious factors (Pazwash, 2011; Butler and Davies, 2004) for each
261 land use type. The difference in WMI was used to indicate the potential for adaptation based on
262 the city plan. For example, a subcatchment with higher positive changes in the WMI indicates
263 that the area is planned to have a land use type with lower imperviousness and therefore is
264 assumed to be more suitable for LID planning, and vice versa.

265

266 3. Results

267 a. Impacts of future climate change on urban flood volumes

268 Figure 3 shows the projected climate change (CC) impacts on urban flooding using the present-
269 day drainage system of the near future (i.e., 2020–2040) under the RCP 8.5 scenario. Without
270 climate change mitigation or adaptation, the TFV was projected to increase significantly with the
271 increase of extreme rainfall events for most of investigated return periods (Table 2). Note that the
272 lower bounds for return periods of 1, 3, and 1000 years fall below the current TFV curve due to
273 the decrease in precipitation intensities. Despite the large uncertainty associated with climate
274 projections, in particular with the 1-, 10-, and 1000-year return periods, the poor service
275 performance of the current system in coping with urban flooding was evident. Overall, the urban
276 flood volume was projected to increase by 52% on average by the multi-model ensemble median
277 by 2020–2040; the largest increase (258%) was projected for the 1-year event and the smallest
278 increase (12%) for the 100-year event.

279

280 b. Benefits of climate change mitigation in reducing urban flood volumes

281 Figure 4 shows the comparison of TFVs under the RCP 8.5 scenario (i.e., a business-as-usual
282 scenario) and the RCP 2.6 scenario (i.e., a climate change mitigation scenario). Although large
283 uncertainties exist arising from climate models, it is clear that the simulated TFVs are much
284 smaller under the RCP 2.6 scenario than under the RCP 8.5 scenario, demonstrating the benefits
285 of climate mitigation in reducing local urban flood volumes. Such benefits are especially evident
286 for floods for smaller return periods. For example, an increase of 936 m³ in flood volume is
287 projected with the increase in 1-year extreme rainfall under the business-as-usual climate change
288 scenario (i.e., RCP 8.5), 52% of which would be reduced if climate change mitigation is in place
289 (i.e., under RCP 2.6). Notably, the peak of the total TFV curve was projected to shift from the 1-
290 year event under the RCP8.5 scenario to the 3-year event under the RCP2.6 scenario (Figure 4b),
291 indicating a substantial reduction in the TFVs (especially at the 1-year return period) (Figure 4c).
292 The lower total TFVs under RCP2.6 scenario could be attributed to the smaller magnitude of
293 rainfall intensity than RCP8.5 scenario (Table 1), demonstrating the important role of climate
294 mitigation in reducing urban flood volumes. Overall, climate change mitigation can reduce future
295 flood volumes by 13% compared to the scenario without mitigation, as indicated by the multi-
296 model ensemble median.

297

298 c. Benefits of adaptation in reducing urban flood volumes

299 Figure 5 shows the overloaded pipelines (red colour) with and without adaptation. The simulated
300 results under the present 3-year event (recommended service level) and 50-year event (one
301 typical extreme event) were selected to illustrate the role of adaptation in coping with floods in
302 the historical period. As shown in Figure 5a, the simulated locations of overloaded pipelines are
303 in good agreement with historical flood points as recorded by local water authorities. Overall, the

304 percentage of overloaded manholes (POM) and the ratio of flood volume (RFV) to input rainfall
305 volume are up to 37% and 35% in the current drainage system (Figure 5a), respectively. When
306 experiencing a 50-year extreme rainfall, the POM and RFV increase to 67% and 38%,
307 respectively. This indicates that current pipe capacities are insufficient to cope with extreme
308 rainfall events (Figure 5b). Spatially, the central portion of the city is the most affected region
309 due to the low service level in the area. With proposed adaptations, urban floods can be reduced
310 to zero under a 3-year flood event. Such benefits of local adaptations are also evident when
311 experiencing more intense precipitation events (e.g., 50-year events), for which the POM and
312 RFV reduced from 67% and 50% to 49% and 17%, respectively.

313

314 Figure 6 shows the future changes in urban flood volume (CTFVs) ($CTFV = (TFV_c - TFV_{nc}) / TFV_{nc}$,
315 where c and nc represent the results with and without climate change, respectively) with changes
316 in extreme rainfall for various return periods. The performance of the current drainage system
317 (no adaptation) was found to be less sensitive to future climate change, as indicated by the flatter
318 slope in Figure 6. For example, a similar magnitude of changes in flood volume was projected
319 given changes in extreme rainfall for the return periods of 3, 50, and 500 years; the CTFV is 0.62,
320 0.32 and 0.35 for these periods, respectively. This is because the capacity of the current system is
321 too small to handle extreme rainfall events with return periods larger than 1 year—a condition
322 under which the current drainage system would be flooded completely, not to mention the
323 situations with increased rainfall intensity in the future. Mathematically, the low sensitivity of
324 the current drainage system to changes in extreme rainfall intensity could be attributed to the
325 large value of the denominator in the calculation of $CTFV$.

326

327 With adaptations in place, the flood volume becomes much smaller than that in the current
328 system due to capacity upgrading to hold more water. For example, when experiencing a 10-year
329 extreme rainfall event, the urban flood volumes for the present period (i.e., TFV_{nc}) are 1041,230,
330 274,650 and 180,610 m³ in the current and two adapted systems, respectively, while in the future
331 period, the magnitude of flood volume (i.e., TFV_c) is relatively similar among the three drainage
332 systems. Therefore, future CTFVs relative to the historical period are much larger in the adapted
333 systems than in the current system. The larger CTFVs in the adapted systems do not mean a
334 worsened drainage system performance. Rather, they imply that the capacity (i.e., service level)
335 of adapted drainage systems tends to become lower with climate change, while the current
336 drainage system has already reached its peak capacity in handling extreme rainfall events in the
337 historical period and thus shows a low sensitivity to future increases in rainfall intensity under
338 climate change scenarios. Notably, the considerable increases in the CTFVs for return periods of
339 less than 10 years in the adapted systems imply that the designed adaptations can effectively
340 attenuate extreme rainfall events for small return periods. For more extreme rainfall events of
341 return periods ≥ 50 years, more consistent results were found for both adaptation scenarios. This
342 indicates that although the performances of adapted drainage systems are significantly improved
343 compared to that of the current system, the flood volume remains large when experiencing
344 extreme rainfall events with return periods larger than 50 years, because flooding in such cases
345 will push the adapted drainage systems to their upper limits.

346

347 d. Climate mitigation versus drainage adaptation

348 Figure 7 shows the reduced TFVs by climate change mitigation and drainage system adaptation
349 as functions of return period. It is evident that both mitigation and adaptation measures are

350 effective in reducing future urban flood volumes. However, such benefits are projected to
351 weaken gradually with the increase in rainfall intensity (i.e., larger return periods). Overall,
352 climate mitigation can lead to a reduction of flood volume by 10-40% compared to the scenario
353 without mitigation. Notably, there are minor negative values of TFV reductions for the return
354 period of 100 and 200 years under climate mitigation scenario. The negative value is attributed to
355 the slightly higher increase in precipitation intensity under climate mitigation scenario (i.e.
356 RCP26) than the scenario without mitigation (i.e. RCP85) simulated by two of five climate
357 models (i.e., GFDL-ESM2m and NorESM1-M, see Table 1), which translated to slightly larger
358 flood volume under climate mitigation scenario. This climate internal variability is partly
359 cancelled by other three climate models, thus leading to very minor negative value by the multi-
360 model ensemble mean. This calls for the use of more climate models (GCMs) to derive more
361 robust projections in the future studies.

362

363 Importantly, our results show that the two adaptation systems proposed in this study are found to
364 be more effective in reducing urban floods than climate change mitigation. In most cases, the
365 benefits of local adaptation are more than double those of mitigation. In extreme cases, the
366 reduction in TFV achieved by adaptation is five times more than that achieved by climate change
367 mitigation (i.e., for the return periods of 2–3 years). Such effectiveness of urban flood reduction
368 through drainage system adaptations has profound implications for local governments charged
369 with managing urban flooding in the future. Notably, the second scenario (LID+pipe) exhibited a
370 higher level of flood volume reduction than the pipe scenario in coping with extreme rainfall
371 events for all investigated return periods. This implies that implementation of LID measures to

372 augment drainage system capacity is more effective through reducing upstream loadings
373 compared to updating the pipe system alone.

374

375 It is noted that local soil characteristics could affect the performance of the designed adaptation
376 systems, in particular the LID measures. However, information about soil properties was not
377 available at the subcatchment level in the study region. Here, a set of sensitivity experiments
378 were conducted by adopting different parameters (e.g., infiltration values) associated with
379 possible soil conditions (i.e., dry sand, loam, and clay soils with little or no vegetation in
380 Supplementary Materials, ST1) for the area. The whiskers in Figure 7 show the uncertainty range
381 arising from the representation of different soil conditions in the drainage model. The benefits of
382 the designed adaptation measures in reducing urban flood volumes were found to be robust
383 regardless of soil conditions, and such benefits exceeded those of climate change mitigation,
384 confirming our major conclusions found in this study.

385

386 4. Uncertainties and Limitations

387 A number of uncertainties and limitations arise from the model structure, parameter inputs,
388 emission scenarios, GCMs, climate downscaling/bias-correction approaches, etc. Specifically,
389 climate projections by GCMs are subject to large uncertainties, in particular regarding
390 precipitation (Covey et al., 2003) at spatial scales, which are relevant for urban flood modelling.

391 An alternative approach is to simulate future climate using a regional climate model (RCM)
392 nested within a GCM. Such climate projections by RCMs have added value in terms of higher
393 spatial resolution, which can provide more detailed regional climate information. However,
394 various levels of bias would still remain in RCM simulations (Teutschbein and Seibert 2012) and

395 bias corrections of RCM projections would be required; e.g., the European project ENSEMBLES
396 (Hewitt and Griggs 2004; Christensen et al. 2008). To run a RCM was not within the scope of
397 this study; instead, we tended to use publicly available climate projections. Here, we obtained the
398 climate projections from the ISI-MIP (Warszawski et al. 2014), which provides spatially
399 downscaled climate data for impact models. The climate projections were also bias-corrected
400 against observations (Hempel et al. 2013) and have been widely used in climate change impact
401 studies on hydrological extremes such as floods and droughts (e.g., Dankers et al. 2014;
402 Prudhomme et al. 2014; Leng et al. 2015a). It should be noted that we used the delta change
403 factor to derive future climate scenarios as inputs into our drainage model instead of using GCM
404 climate directly. This is because the relative climate change signal simulated by GCMs is argued
405 to be more reliable than the simulated absolute values (Ho et al. 2012). Moreover, we used an
406 ensemble of GCM simulations rather than one single climate model in order to characterise the
407 uncertainty range arising from climate projections. However, disadvantages of this method are
408 that transient climate changes cannot be represented and that changes in intra-seasonal or daily
409 climate variability are not taken into account (Leng and Tang, 2014). Such sources of uncertainty
410 can be explored when improved climate models at finer scales become available (Jaramillo and
411 Nazemi 2017).

412

413 In addition, the SIF parameters were assumed to remain stable in the future and only changes in
414 the daily mean intensity were considered, because future sub-hourly climate projections were not
415 readily available. The full climate variability range would also be under-sampled, although we
416 used five climate models to show the possible range. Given the above limitations, we
417 acknowledge that the modelling results represent the first-order potential climate change impacts

418 on urban floods. Future efforts should be devoted to the representation of dynamic rainfall
419 changes at hourly time steps with consideration of non-stationary climate change.

420

421 Moreover, several assumptions had to be made due to limitations of the current modelling
422 structure and approach. For example, the conveyance capacities of the drainage system and flood
423 volume would largely depend on the state of drainage systems. Hence, a drainage system
424 obstructed by vegetation, waste, or artefacts (cables, pipes, temporary constructions) can make
425 the outcomes of the SWMM calculation significantly different from observations. However,
426 quantifying the impacts of drainage system states on urban flood volumes is not trivial because
427 of the difficulties involved in collecting field data and selecting and using appropriate methods
428 for reasonable assessment of pipe conditions (Ana and Bauwens, 2007; Fenner, 2000), and was
429 not within the scope of this study. With deterioration, such as ageing network, pipe deterioration,
430 blockage, and construction failures, drainage systems were shown to become more vulnerable to
431 extreme rainfalls as demonstrated in previous studies (Dawson et al., 2008; CIRIA, 1997; Davies
432 et al., 2001). It is very likely that our simulated urban flood volumes would be underestimated
433 without considering the changes in drainage conditions (Pollert et al., 2005).

434

435 Further, constrained by the one-dimensional modelling approach using SWMM, the
436 performances of LID measures were mainly evaluated according to their effects in reducing
437 water volume from overloaded manholes (Oraei Zare et al., 2012; Lee et al., 2013). That is, the
438 LID adaptation measure was mainly designed to reduce the amount of water rather than slowing
439 down the water speed, which has been demonstrated to be effective in reducing urban floods
440 (Messner et al., 2006; Ashley et al., 2007; Floodsite, 2009). However, it should be noted that

441 most LID measures can reduce runoff volume and flow speed at the same time, although some of
442 the LID measures are primarily designed to slow down the flow speed, i.e., vegetated swales. To
443 examine whether flood retention of a given event is induced by runoff volume or the internal
444 speed control function in the model is difficult and requires detailed data for model validations.
445 Specifically, the required information about surface roughness, soil conductivity, and seepage
446 rate were unavailable at the subcatchment scale in the study region. Therefore, a simplified
447 modelling approach was used to take advantage of existing data, especially for the design of LID
448 measures. With the aid of more detailed field data and planning documents, the design of LID
449 measures could be significantly improved by implementing more advanced approaches (Elliott
450 and Trowsdale, 2007; Zoppou, 2001).

451

452 Evaluation of other potential adaptation strategies, such as flood retention by rain gardens and
453 green roofs, can be explored in the future to gain additional insights into the performance of LID
454 systems. In particular, the cost-effectiveness of the proposed adaptation measures should be
455 accounted for. Indeed, a major limitation of this study is lack of assessment of costs and benefits
456 of adaptation measures from the economic perspective. In fact, besides the effectiveness of
457 proposed adaptation measures in reducing flood volume, assessment of the associated economic
458 costs is essential for flood risk management (Rojas et al., 2013; Veith et al., 2003; Hinkel et al.,
459 2014; Aerts et al., 2014; Ward et al., 2017). For example, Ward et al. (2017) showed that
460 investments in urban flood protections with dykes are not economically attractive everywhere.
461 Higher investment and maintenance costs may prohibit the implementation of adaptation
462 strategies as proposed in this study. Future efforts should therefore be devoted to building a
463 framework for assessing the costs and benefits of urban flood reduction measures and examine

464 whether the reduced losses are higher than the costs of investments and maintenance of these
465 measures.

466

467 Nevertheless, given these limitations, this study stands out from previous climate impact
468 assessment studies of urban flood volumes by having proposed two feasible adaptation strategies
469 and compared their benefits to those from global-scale climate change mitigations through GHG
470 reductions within a consistent framework. Depending on the progress on data collection and the
471 demands of local authorities, more advanced methods for pipe assessment (e.g., considering the
472 changing pipe conditions), LID measures (detailed modelling of LID control), and two-
473 dimensional surface flooding for assessment of flood damage and risk are planned in a future
474 study to provide a more comprehensive analysis of the adaptation measures.

475

476 5. Summary and Conclusions

477 The potential impacts of future climate change on current urban drainage systems have received
478 increasing attention during recent decades because of the devastating impacts of urban flooding
479 on the economy and society (Chang et al., 2013; Zhou et al., 2012; Abdellatif et al., 2015).
480 However, few studies have explored the role of both climate change mitigation and drainage
481 adaptations in coping with urban flooding in a changing climate. This study investigated the
482 performance of a drainage system in a typical city in Northern China in response to various
483 future scenarios. In particular, we assessed the potential changes in urban flood volume and
484 explored the role of both mitigation and adaptation in reducing urban flood volumes in a
485 consistent manner.

486

487 Our results show significant increases in urban flood volumes due to increases in precipitation
488 extremes, especially for return periods of less than 10 years. Overall, urban flood volume in the
489 study region is projected to increase by 52% by the multi-model ensemble median in the period
490 of 2020–2040. Such increases in flood volume can be reduced considerably by climate change
491 mitigation through reduction of GHG emissions. For example, the future TFVs under 1-year
492 extreme rainfall events can be reduced by 50% when climate change mitigation is in place.
493 Besides global-scale climate change mitigation, regional/local adaptation can be implemented to
494 cope with the adverse impacts of future climate change on urban flood volumes. Here, the
495 adaptation measures as designed in this study were demonstrated to be much more effective in
496 reducing future flood volumes than climate change mitigation measures. In general, the reduced
497 flood volumes achieved by adaptation were more than double those achieved by climate change
498 mitigation.

499

500 Through a comprehensive investigation of future urban floods, this study provides much-needed
501 insights into urban flood management for similar urban areas in China, most of which are
502 equipped with highly insufficient drainage capacities. By comparing the reduction of flood
503 volume by climate change mitigation (via reduction of GHG emissions) and local adaptation (via
504 improvement of drainage systems), this study highlights the effectiveness of system adaptations
505 in reducing future flood volumes. This has important implications for the research community
506 and decision-makers involved in urban flood management. We emphasise the importance of
507 accounting for both global-scale climate change mitigation and local-scale adaptation in
508 assessing future climate impacts on urban flood volumes within a consistent framework.

509

510 **Acknowledgements**

511 This research was supported by the Public Welfare Research and Ability Construction Project of
512 Guangdong Province, China (Grant No. 2017A020219003), the Water Conservancy Science and
513 Technology Innovation Project of Guangdong province, China (Grant No. 201710), the Natural
514 Science Foundation of Guangdong Province, China (No. 2014A030310121) and the Scientific
515 Research Foundation for the Returned Overseas Chinese Scholars, State Education Ministry. G.
516 Leng and M. Huang were supported by the Integrated Assessment Research program through the
517 Integrated Multi-sector, Multi-scale Modeling (IM³) Scientific Focus Area (SFA) sponsored by
518 the Biological and Environmental Research Division of Office of Science, U.S. Department of
519 Energy. The Pacific Northwest National Laboratory (PNNL) is operated for the U.S. DOE by
520 Battelle Memorial Institute under contract DE-AC05-76RL01830

521 **References**

- 522 Abdellatif, M., Atherton, W., Alkhaddar, R., and Osman, Y.: Flood risk assessment for urban water
523 system in a changing climate using artificial neural network, *Natural Hazards*, 79, 1059-1077, 2015.
- 524 Aerts, J. C., Botzen, W. W., Emanuel, K., Lin, N., de Moel, H., & Michel-Kerjan, E. O. (2014).
525 Evaluating flood resilience strategies for coastal megacities. *Science*, 344(6183), 473-475.
- 526 Akan, O. A.: *Urban stormwater hydrology: a guide to engineering calculations*, CRC Press, 1993.
- 527 Alfieri, L., Feyen, L., and Di Baldassarre, G.: Increasing flood risk under climate change: a pan-European
528 assessment of the benefits of four adaptation strategies, *Climatic Change*, 136, 507-521, 10.1007/s10584-
529 016-1641-1, 2016.
- 530 Ana, E., and Bauwens, W.: Sewer network asset management decision-support tools: a review,
531 *International Symposium on New Directions in Urban Water Management*, 12-14 September 2007,
532 UNESCO Paris, 2007.
- 533 Apel, H., Aronica, G. T., Kreibich, H., and Thielen, A. H.: Flood risk analyses-how detailed do we need
534 to be?, *Natural Hazards*, 49, 79-98, 2009.
- 535 Arnbjerg-Nielsen, K.: Quantification of climate change effects on extreme precipitation used for high
536 resolution hydrologic design, *Urban Water Journal*, 9, 57-65, 2012.
- 537 Arnbjerg-Nielsen, K., Leonardsen, L., and Madsen, H.: Evaluating adaptation options for urban flooding
538 based on new high-end emission scenario regional climate model simulations, *Clim. Res.*, 64, 73-84,
539 10.3354/cr01299, 2015.

540 Ashley, R., Garvin, S., Pasche, E., Vassilopoulos, A., and Zevenbergen, C.: Advances in Urban Flood
541 Management, in, edited by: Ashley, R., Garvin, S., Pasche, E., Vassilopoulos, A., and Zevenbergen, C.,
542 Taylor & Francis/Balkema, London, UK, 2007.

543 Ashley, R. M., Balmforth, D. J., Saul, A. J., and Blanskby, J. D.: Flooding in the future - predicting
544 climate change, risks and responses in urban areas, *Water Science and Technology*, 52, 265-273, 2005.

545 Berggren, K., Packman, J., Ashley, R., and Viklander, M.: Climate changed rainfalls for urban drainage
546 capacity assessment, *Urban Water Journal*, 11, 543-556, 10.1080/1573062X.2013.851709, 2014.

547 Butler, D., and Davies, J.: *Urban drainage*, Third Edition, CRC Press, London. ISBN: 0415455251, 2010.

548 *China Statistical Yearbook: National Bureau of Statistics of China*, China Statistics Press, Beijing, 2015.

549 Chang, H. K., Tan, Y. C., Lai, J. S., Pan, T. Y., Liu, T. M., and Tung, C. P.: Improvement of a drainage
550 system for flood management with assessment of the potential effects of climate change, *Hydrological
551 Sciences Journal*, 58, 2013.

552 Chow, V. T., Maidment, D. R., and Mays, L. W.: *Applied Hydrology*, 2nd Edition, in, McGraw-Hill,
553 New York. ISBN: 007174391X, 2013.

554 CIRIA: *Risk Management for Real Time Control in Urban Drainage Systems: Scoping Study*, Project
555 Report 45. CIRIA, London., 1997.

556 Coles S, *An Introduction to Statistical Modeling of Extreme Values*, Springer Series in Statistics
557 (Springer, London), 2001.

558 Covey, C., et al.: An overview of results from the Coupled Model Intercomparison Project, *Global and
559 Planetary Change*, 37(1), 103-133, 2003.

560 Dankers, R., et al.: First look at changes in flood hazard in the Inter-Sectoral Impact Model
561 Intercomparison Project ensemble, *Proceedings of the National Academy of Sciences*, 111(9), 3257-3261,
562 2014.

563 Davies, J. P., Clarke, B. A., Whiter, J. T., and Cunningham, R. J.: Factors influencing the structural
564 deterioration and collapse of rigid sewer pipes, *Urban Water*, 3, 73-89, 2001.

565 Dawson, R. J., Speight, L., Hall, J. W., Djordjevic, S., Savic, D., and Leandro, J.: Attribution of flood risk
566 in urban areas, *Journal of Hydroinformatics*, 10, 275-288, 2008.

567 Ding, Y., Ren, G., Shi, G., Gong, P., Zheng, X., Zhai, P., Zhang, D., Zhao, Z., Wang, S., Wang, H., Luo,
568 Y., Chen, D., Gao, X., and Dai, X.: National assessment report of climate change (I): climate change in
569 China and its future trend. *Adv Clim Change Res* 2:3–8 (in Chinese), 2006.

570 Elliott, A. H., and Trowsdale, S. A.: A review of models for low impact urban stormwater drainage,
571 *Environmental Modelling & Software*, 22, 394-405, 2007.

572 Elliott, J., et al.: Constraints and potentials of future irrigation water availability on agricultural
573 production under climate change, *Proceedings of the National Academy of Sciences*, 111, 3239–3244,
574 2014.

575 Fenner, R. A.: Approaches to sewer maintenance: a review, *Urban Water*, 2, 343-356, 2000.

576 Floodsite: Flood risk assessment and flood risk management. An introduction and guidance based on
577 experiences and findings of FLOODsite (an EU-funded Integrated Project), Deltares|Delft Hydraulics.
578 ISBN 978 90 8 |4067|0, 2009.

579 Haddeland, I., et al.: Global water resources affected by human interventions and climate change,
580 *Proceedings of the National Academy of Sciences*, 111, 3251–3256, 2014.

581 Hempel, S., Frieler, K., Warszawski, L., Schewe, J., and Piontek, F.: A trend-preserving bias correction–
582 the ISI-MIP approach, *Earth System Dynamics*, 4(2), 219-236, 2013.

583 Hinkel, J., Lincke, D., Vafeidis, A. T., Perrette, M., Nicholls, R. J., Tol, R. S., ... & Levermann, A. (2014).
584 Coastal flood damage and adaptation costs under 21st century sea-level rise. *Proceedings of the National
585 Academy of Sciences*, 111(9), 3292-3297.

586 Horritt, M. S., and Bates, P. D.: Evaluation of 1D and 2D numerical models for predicting river flood
587 inundation, *Journal of Hydrology*, 268, 87-99, 2002.

588 Ho, C. K., Stephenson, D. B., Collins, M., Ferro, C. A., and Brown, S. J.: Calibration strategies: a source
589 of additional uncertainty in climate change projections, *Bulletin of the American Meteorological Society*,
590 93(1), 21-26, 2012.

591 Jaramillo, P., and Nazemi, A.: *Assessing Urban Water Security under Changing Climate: Challenges and
592 Ways Forward*. Sustainable Cities and Society, 2017.

593 Karamouz, M., Nazif, S., and Zahmatkesh, Z.: Self-Organizing Gaussian-Based Downscaling of Climate
594 Data for Simulation of Urban Drainage Systems, *Journal of Irrigation Drainage Engineering*, 139, 98-112,
595 2013.

596 Katz, R. W., Parlange, M. B., Naveau, P.: Statistics of extremes in hydrology, *Advances in Water
597 Resources*, 25, 1287–1304, 2002.

598 Larsen, A. N., Gregersen, I. B., Christensen, O. B., Linde, J. J., and Mikkelsen, P. S.: Potential future
599 increase in extreme one-hour precipitation events over Europe due to climate change, *Water Science and
600 Technology*, 60, 2205-2216, 2009.

601 Lee, J. M., Hyun, K. H., and Choi, J. S.: Analysis of the impact of low impact development on runoff
602 from a new district in Korea, *Water Science and Technology*, 68, 1315-1321,, 2013.

603 Leng, G., and Tang, Q.: Modeling the impacts of future climate change on irrigation over China:
604 Sensitivity to adjusted projections, *Journal of Hydrometeorology*, 15(5), 2085-2103, 2014.

605 Leng, G., Tang, Q., and Rayburg, S.: Climate change impacts on meteorological, agricultural and
606 hydrological droughts in China, *Global and Planetary Change*, 126, 23-34, 2015a.

607 Leng, G., Huang, M., Tang, Q., and Leung, L. R.: A modeling study of irrigation effects on global surface
608 water and groundwater resources under a changing climate, *Journal of Advances in Modeling Earth
609 Systems*, 7(3), 1285-1304, 2015b.

610 Messner, F., Penning-Rowsell, E., Green, C., Meyer, V., Tunstall, S., and Van der Veen, A.: Guidelines
611 for Socio-economic Flood Damage Evaluation, Report Nr. T9-06-01, in, FLOOD site, HR Wallingford,
612 UK, 2006.

613 Mishra, A.: A study on the occurrence of flood events over Jammu and Kashmir during September 2014
614 using satellite remote sensing, *Natural Hazards*, 78, 1463-1467, 2015.

615 MOHURD: AQSIQ. Code for Design of Outdoor Wastewater Engineering (GB 50014-2006), Ministry of
616 Housing and Urban-Rural Development, General Administration of Quality Supervision, Inspection and
617 Quarantine of the People’s Republic of China: Beijing, China (In Chinese), 2011.

618 MOHURD: Technical Guidelines for Establishment of Intensity-Duration-Frequency Curve and Design
619 Rainstorm Profile (In Chinese), Ministry of Housing and Urban-Rural Development of the People's
620 Republic of China and China Meteorological Administration, 2014.

621 Moore, T. L., Gulliver, J. S., Stack, L., and Simpson, M. H.: Stormwater management and climate change:
622 vulnerability and capacity for adaptation in urban and suburban contexts, *Climatic Change*, 138, 491-504,
623 10.1007/s10584-016-1766-2, 2016.

624 Notaro, V., Liuzzo, L., Freni, G., and La Loggia, G.: Uncertainty Analysis in the Evaluation of Extreme
625 Rainfall Trends and Its Implications on Urban Drainage System Design, *Water*, 7, 6931-6945, 2015.

626 Olsen, A., Zhou, Q., Linde, J., and Arnbjerg-Nielsen, K.: Comparing Methods of Calculating Expected
627 Annual Damage in Urban Pluvial Flood Risk Assessments, *Water*, 7, 255-270, 2015.

628 Olsson, J., Berggren, K., Olofsson, M., and Viklander, M.: Applying climate model precipitation
629 scenarios for urban hydrological assessment: A case study in Kalmar City, Sweden, *Atmospheric
630 Research*, 92, 364-375, <http://dx.doi.org/10.1016/j.atmosres.2009.01.015>, 2009.

631 Oraei Zare, S., Saghafian, B., Shamsai, A., and Nazif, S.: Multi-objective optimization using evolutionary
632 algorithms for qualitative and quantitative control of urban runoff, *Hydrology and Earth System Sciences*,
633 9, 777-817, 2012.

634 Pazwash, H.: *Urban Storm Water Management*, CRC Press, Taylor and Francis, Boca Raton, FL, 2011.

635 Peng, H. Q., Liu, Y., Wang, H. W., and Ma, L. M.: Assessment of the service performance of drainage
636 system and transformation of pipeline network based on urban combined sewer system model,
637 *Environmental Science And Pollution Research*, 22, 15712-15721, 2015.

638 Piani, C., Weedon, G. P., Best, M., Gomes, S. M., Viterbo, P., Hagemann, S., and Haerter, J. O.:
639 Statistical bias correction of global simulated daily precipitation and temperature for the application of
640 hydrological models, *Journal of Hydrology*, 395, 199–215, 2010.

641 Piontek, F., et al.: Multisectoral climate impact hotspots in a warming world, *Proceedings of the National
642 Academy of Sciences*, 111(9), 3233-3238, 2014.

643 Pollert, J., Ugarelli, R., Saegrov, S., Schilling, W., and Di Federico, V.: The hydraulic capacity of
644 deteriorating sewer systems, *Water Science and Technology*, 52, 207-214, 2005.

645 Poussin, J. K., Bubeck, P., Aerts, J., and Ward, P. J.: Potential of semi-structural and non-structural
646 adaptation strategies to reduce future flood risk: case study for the Meuse, *Natural Hazards and Earth
647 System Sciences*, 12, 3455-3471, 2012.

648 Prudhomme, C., et al.: Hydrological droughts in the 21st century, hotspots and uncertainties from a global
649 multimodel ensemble experiment, *Proceedings of the National Academy of Sciences*, 111(9), 3262-3267,
650 2014.

651 Rojas, R., Feyen, L., and Watkiss, P.: Climate change and river floods in the European Union: Socio-
652 economic consequences and the costs and benefits of adaptation, *Global Environmental Change-Human
653 and Policy Dimensions*, 23, 1737-1751, [10.1016/j.gloenvcha.2013.08.006](https://doi.org/10.1016/j.gloenvcha.2013.08.006), 2013.

654 Rossman, L. A., and Huber, W. C.: *Storm Water Management Model Reference Manual EPA/600/R-
655 15/162A*, 2016.

656 Veith, T. L., Wolfe, M. L., and Heatwole, C. D.: Optimization procedure for cost effective BMP
657 placement at a watershed scale, *Journal of the American Water Resources Association*, 39, 1331-1343,
658 [10.1111/j.1752-1688.2003.tb04421.x](https://doi.org/10.1111/j.1752-1688.2003.tb04421.x), 2003.

659 Vojinovic, Z., and Tutulic, D.: On the use of 1D and coupled 1D-2D modelling approaches for
660 assessment of flood damage in urban areas, *Urban Water Journal*, 6, 183-199, 2009.

661 Ward, P. J., Jongman, B., Aerts, J. C., Bates, P. D., Botzen, W. J., Loaiza, A. D., ... & Winsemius, H. C.
662 (2017). A global framework for future costs and benefits of river-flood protection in urban areas. *Nature
663 Climate Change*. 7, 642–646.

664 Warszawski, L. et al.: The Inter-Sectoral Impact Model Intercomparison Project [ISI-MIP]: Project
665 framework, *Proceedings of the National Academy of Sciences*, 111(9), 3228–3232, 2014.

666 Willems, P., Arnbjerg-Nielsen, K., Olsson, J., and Nguyen, V. T. V.: Climate change impact assessment
667 on urban rainfall extremes and urban drainage: Methods and shortcomings, *Atmospheric Research*, 103,
668 106-118, 2012.

669 Willems, P.: Revision of urban drainage design rules after assessment of climate change impacts on
670 precipitation extremes at Uccle, Belgium, *Journal of Hydrology*, 496, 166-177, 2013.

671 Yang, G.: Historical change and future trends of storm surge disaster in China's coastal area. *Journal of*
672 *Natural Disasters* 9, 23-30 (in Chinese), 2000.

673 Wu, H., Huang, G., Meng, Q., Zhang, M., and Li, L.: Deep Tunnel for Regulating Combined Sewer
674 Overflow Pollution and Flood Disaster: A Case Study in Guangzhou City, China, *Water*, 8, 329, 2016.

675 Yazdanfar, Z., and Sharma, A.: Urban drainage system planning and design-challenges with climate
676 change and urbanization: a review, *Water Science & Technology*, 72, 165-179, 2015.

677 Yin, J., Yu, D. P., Yin, Z., Liu, M., and He, Q.: Evaluating the impact and risk of pluvial flash flood on
678 intra-urban road network: A case study in the city center of Shanghai, China, *Journal of Hydrology*, 537,
679 138-145, 2016.

680 Zahmatkesh, Z., Karamouz, M., Goharian, E., and Burian, S. J.: Analysis of the Effects of Climate
681 Change on Urban Storm Water Runoff Using Statistically Downscaled Precipitation Data and a Change
682 Factor Approach, *Journal of Hydrologic Engineering*, 20, 11, 2015.

683 Zhang, B., and Guan, Y.: *Watersupply & Drainage Design Handbook*, China Construction Industry Press,
684 ISBN: 9787112136803, Beijing, China, 2012.

685 Zhang, Y.-q., Lv, M., and Wang, Q.-g.: Formula method design of drainage pipe network and analysis of
686 model simulation, *Water Resour. Power*, 33, 105-107, 2015.

687 Zhang, D., Zhao, D. q., Chen, J. n., and Wang, H. z.: Application of Chicago approach in urban drainage
688 network modeling, *Water & Wastewater Engineering*, 34, 354-357, 2008.

689 Zhou, Q., Mikkelsen, P. S., Halsnaes, K., and Arnbjerg-Nielsen, K.: Framework for economic pluvial
690 flood risk assessment considering climate change effects and adaptation benefits, *Journal of Hydrology*,
691 414, 539-549, 2012.

692 Zhou, Q., Panduro, T., Thorsen, B., and Arnbjerg-Nielsen, K.: Adaption to Extreme Rainfall with Open
693 Urban Drainage System: An Integrated Hydrological Cost-Benefit Analysis, *Environmental Management*,
694 51, 586-601, 2013.

695 Zhou, Q., Ren, Y., Xu, M., Han, N., and Wang, H.: Adaptation to urbanization impacts on drainage in the
696 city of Hohhot, China, *Water Science and Technology*, 73, 167-175, 10.2166/wst.2015.478, 2016.

697 Zoppou, C.: Review of urban storm water models, *Environmental Modelling & Software*, 16, 195-231,
698 2001.

699 **Table 1** Projected changes in precipitation intensity under return periods ranging from 1 year to 1000
700 years by five Global Climate Models under two Representative Concentration Pathways (RCPs)

		1	2	3	10	20	50	100	200	500	1000
GFDL- ESM2M	RCP8.5	2.12	1.23	1.34	1.25	1.27	1.21	1.08	1.12	1.24	1.23
	RCP2.6	1.74	1.08	1.03	1.11	1.07	1.15	1.14	1.15	1.19	1.16
HadGE M2-ES	RCP8.5	0.62	1.08	1.09	1.06	1.01	1.03	1.17	1.26	1.23	1.14
	RCP2.6	0.36	1.2	1.19	1.04	1.02	1.11	1.31	1.26	1.37	1.24
IPSL- CM5A- LR	RCP8.5	1.44	1.17	1.28	1.17	1.08	1.09	1.02	1.1	1.12	1.13
	RCP2.6	0.74	1.04	1.18	1.01	1.06	1.03	1.01	0.99	0.95	1
MIROC -ESM- CHEM	RCP8.5	2.13	1.38	1.3	1.51	1.32	1.23	1.17	1.27	1.16	1.31
	RCP2.6	0.71	1.12	1.14	1.18	1.1	1.07	1.01	1.09	1.01	1.09
NorES M1-M	RCP8.5	2.11	0.96	0.8	1.63	1.35	1.15	1.08	1.01	1.04	0.97
	RCP2.6	0.11	1.09	1.05	1.28	1.17	1.08	1.1	1.18	1.09	1.2

701

702 **List of Figures**

703 **Figure 1** Land use of the study region for the year 2010 (a) and 2020 (b). Pipe network
704 description of current and planned drainage systems (c). Difference in Weighted Mean
705 Imperviousness (WMI) between year 2010 and 2020 (d).

706 **Figure 2** Illustration of total flood volume (TFVs) as a function of return periods (a) and
707 estimation of average total expected TFVs per year (i.e., the grey area in b) under a stationary
708 drainage system.

709 **Figure 3** Changes in total flood volume (TFV) as a function of precipitation intensity at various
710 return periods under RCP8.5 scenario without mitigation and adaptation. Red solid line
711 represents the multi-model ensemble median TFV with shaded areas denoting the ensemble
712 range. Red dashed line is the TFV under present condition. Box plots show the relative changes
713 in TFV by 2020–2040 relative to present condition. Box edges illustrate the 25th and 75th
714 percentile, the central mark is the median and whiskers mark the 5th and 95th percentiles.

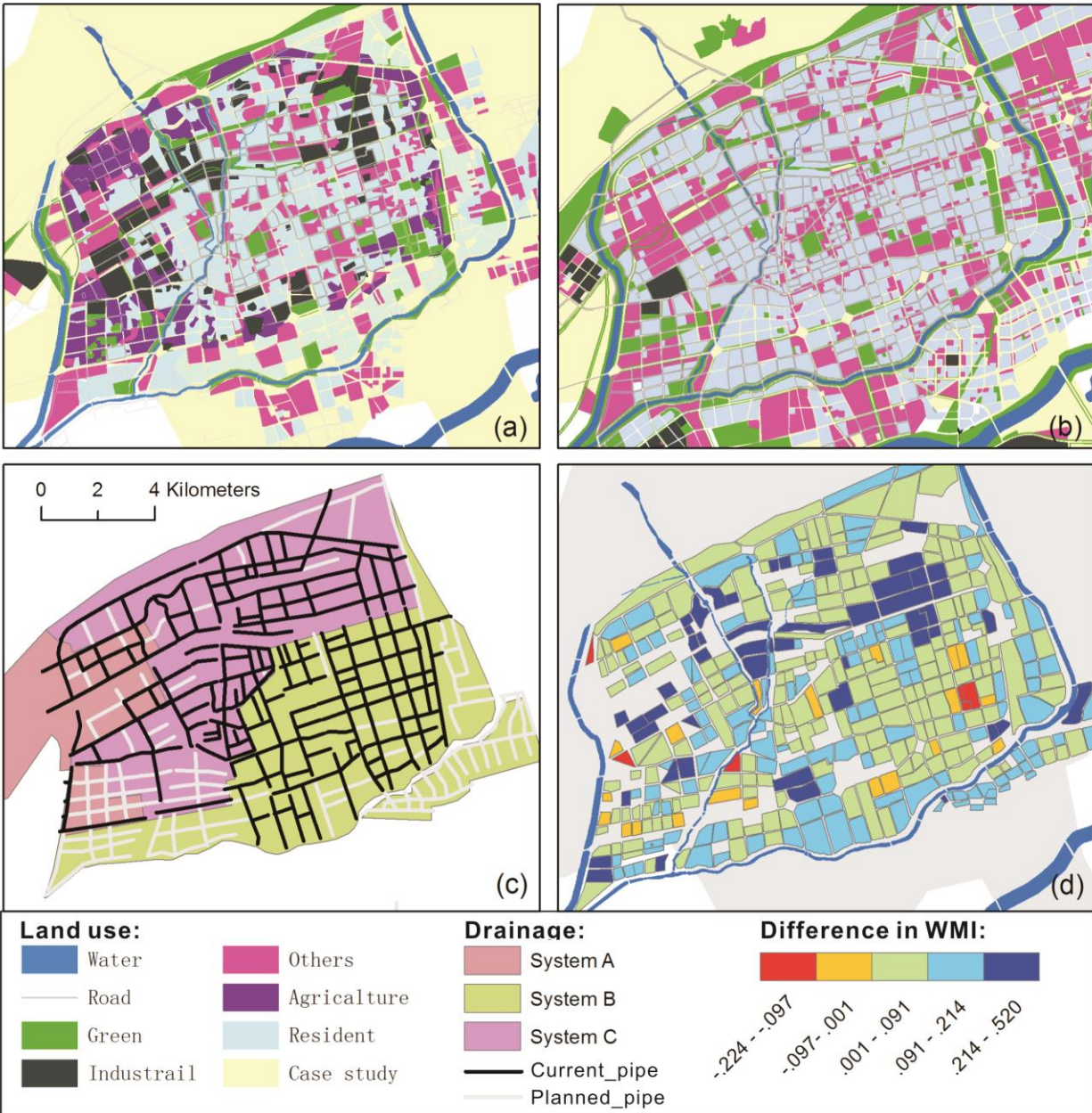
715 **Figure 4** Comparison of (a) flood volume, (b) total TFVs (i.e., the piece-wise integral of flood
716 volume versus the expected frequency with changes in precipitation intensity of various return
717 periods under RCP8.5 (blue) and RCP2.6 (red). (c) is the TFV reduction calculated as the
718 percentage difference in TFVs under RCP2.6 compared to RCP8.5 (i.e., benefits of climate
719 mitigation) at various return periods.

720 **Figure 5** Spatial distribution of overloaded pipelines (red colour) induced by the 3-year (left
721 column) and 50-year extreme events (right column) without and with adaptations. The total
722 percentage of overloaded manholes (POM) and ratio of flood volume (RFV) to input rainfall
723 volume are summarised for each scenario. Historical flood points and local land use, mainly the
724 traffic network and green spaces, are shown in (a).

725 **Figure 6** Future changes in flood volumes (CTFVs) relative to historical conditions under the
726 current drainage system (yellow) and two adaptation scenarios (i.e., Pipe in red and Pipe+LID in
727 green) at various return periods.

728 **Figure 7** Comparison of benefits of climate mitigation and two adaptation strategies in reducing
729 urban flood volumes with changes in precipitation intensities for various return periods, and with
730 related variations (boundary bars) as a result of uncertainty arising from local soil conditions.

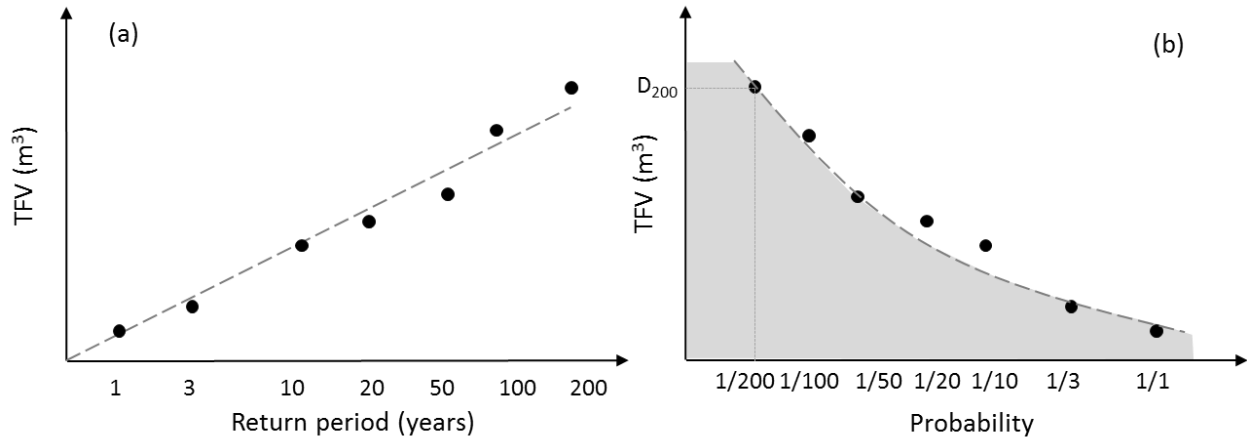
731



732

733 **Figure 1** Land use of the study region for the year 2010 (a) and 2020 (b). Pipe network
 734 description of current and planned drainage systems (c). Difference in Weighted Mean
 735 Imperviousness (WMI) between year 2010 and 2020 (d).

736

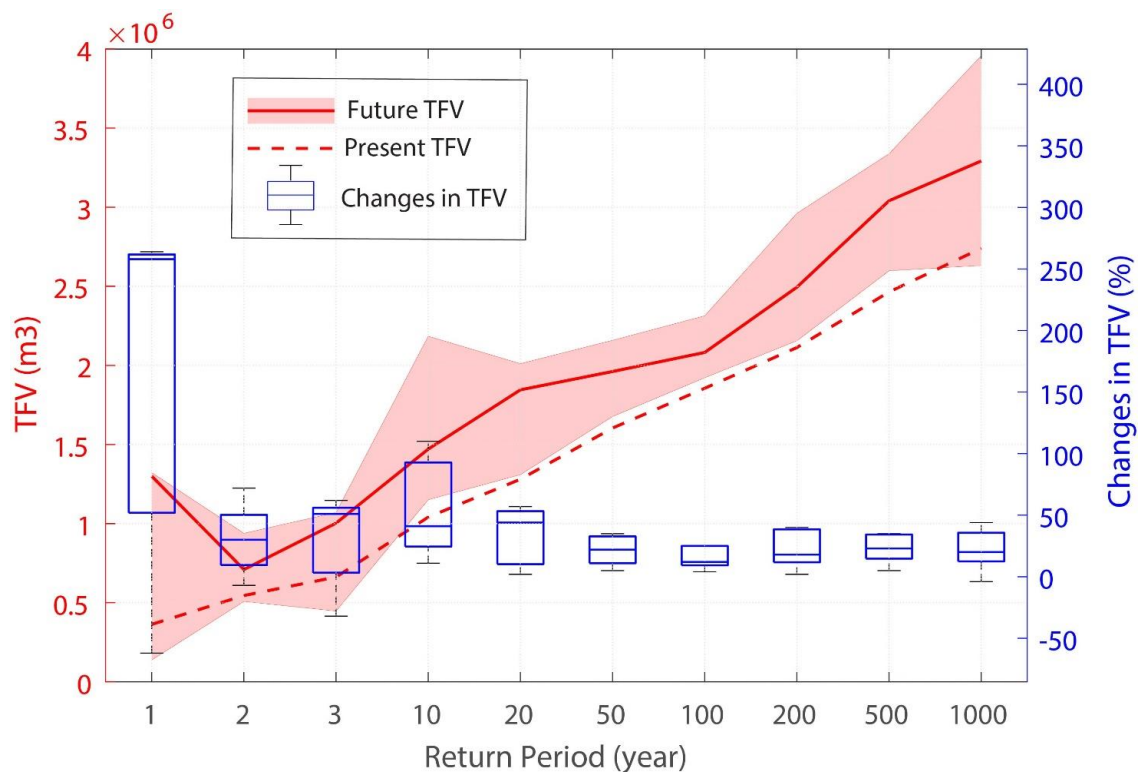


737

738 **Figure 2** Illustration of total flood volume (TFVs) as a function of return periods (a) and
 739 estimation of average total expected TFVs per year (i.e., the grey area in b) under a stationary
 740 drainage system.

741

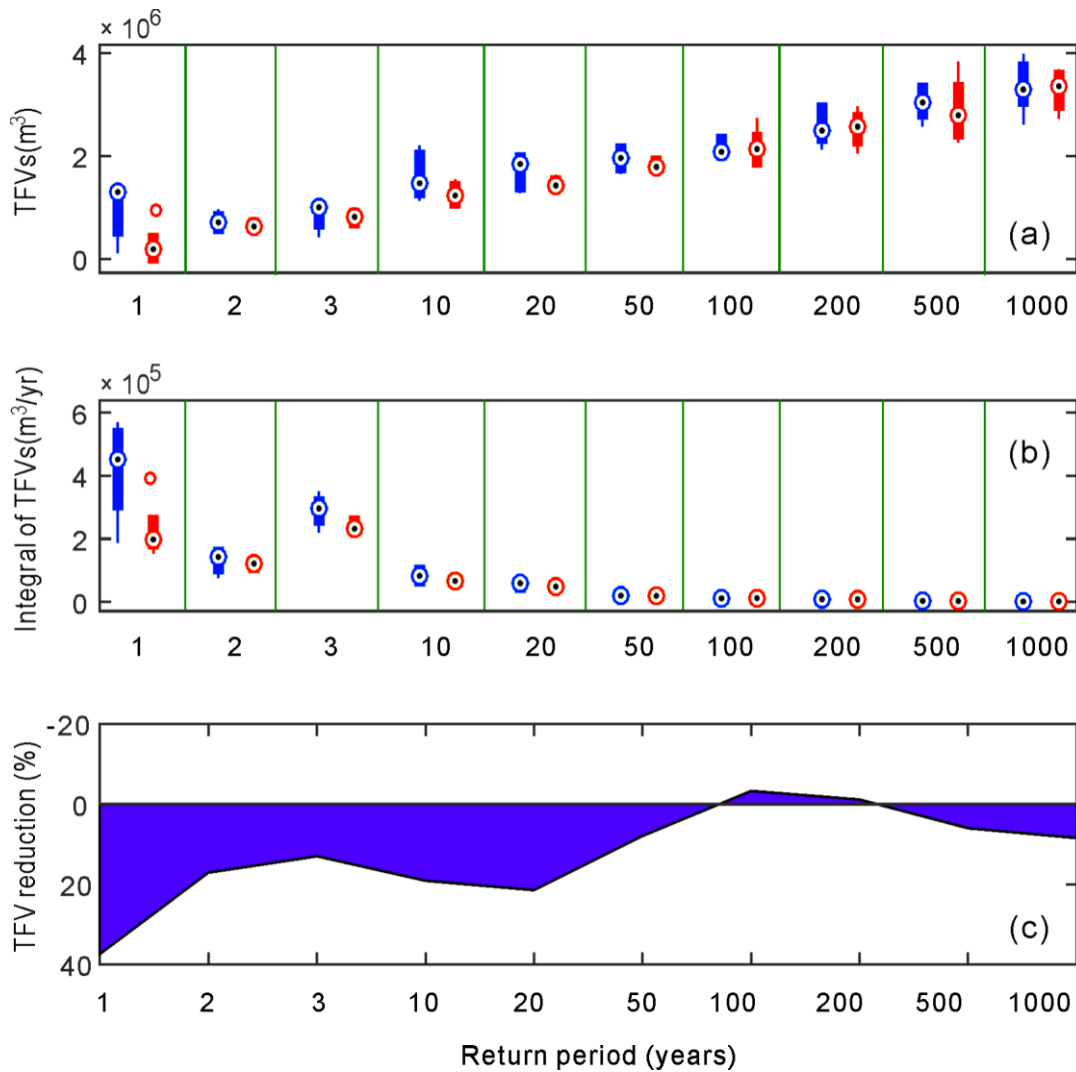
742



743

744 **Figure 3** Changes in total flood volume (TFV) as a function of precipitation intensity at various
745 return periods under RCP8.5 scenario without mitigation and adaptation. Red solid line
746 represents the multi-model ensemble median TFV with shaded areas denoting the ensemble
747 range. Red dashed line is the TFV under present condition. Box plots show the relative changes
748 in TFV by 2020–2040 relative to present condition. Box edges illustrate the 25th and 75th
749 percentile, the central mark is the median and whiskers mark the 5th and 95th percentiles.

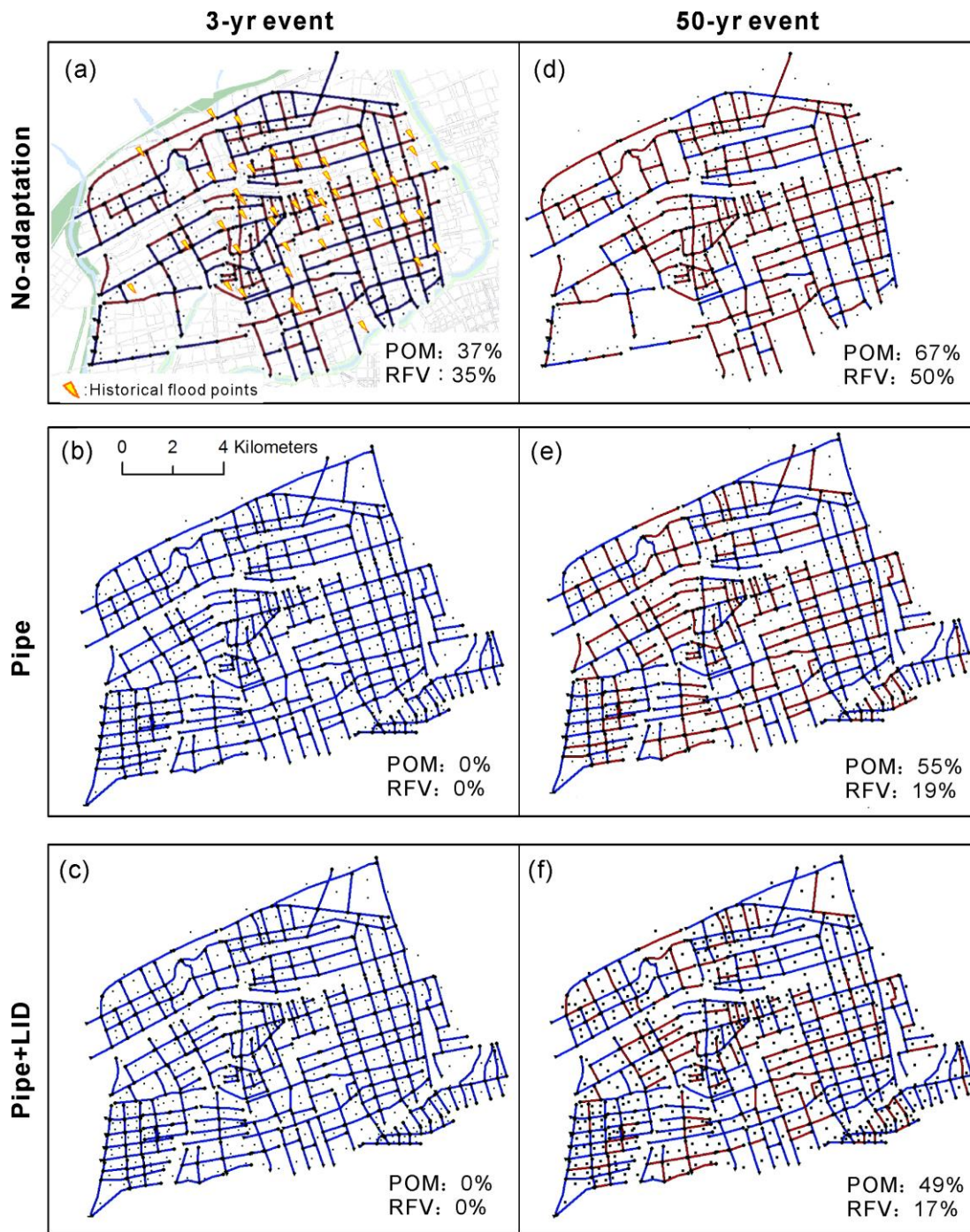
750



751

752 **Figure 4** Comparison of (a) flood volume, (b) total TFVs (i.e., the piece-wise integral of flood
 753 volume versus the expected frequency with changes in precipitation intensity of various return
 754 periods under RCP8.5 (blue) and RCP2.6 (red). (c) is the TFV reduction calculated as the
 755 percentage difference in TFVs under RCP2.6 compared to RCP8.5 (i.e., benefits of climate
 756 mitigation) at various return periods.

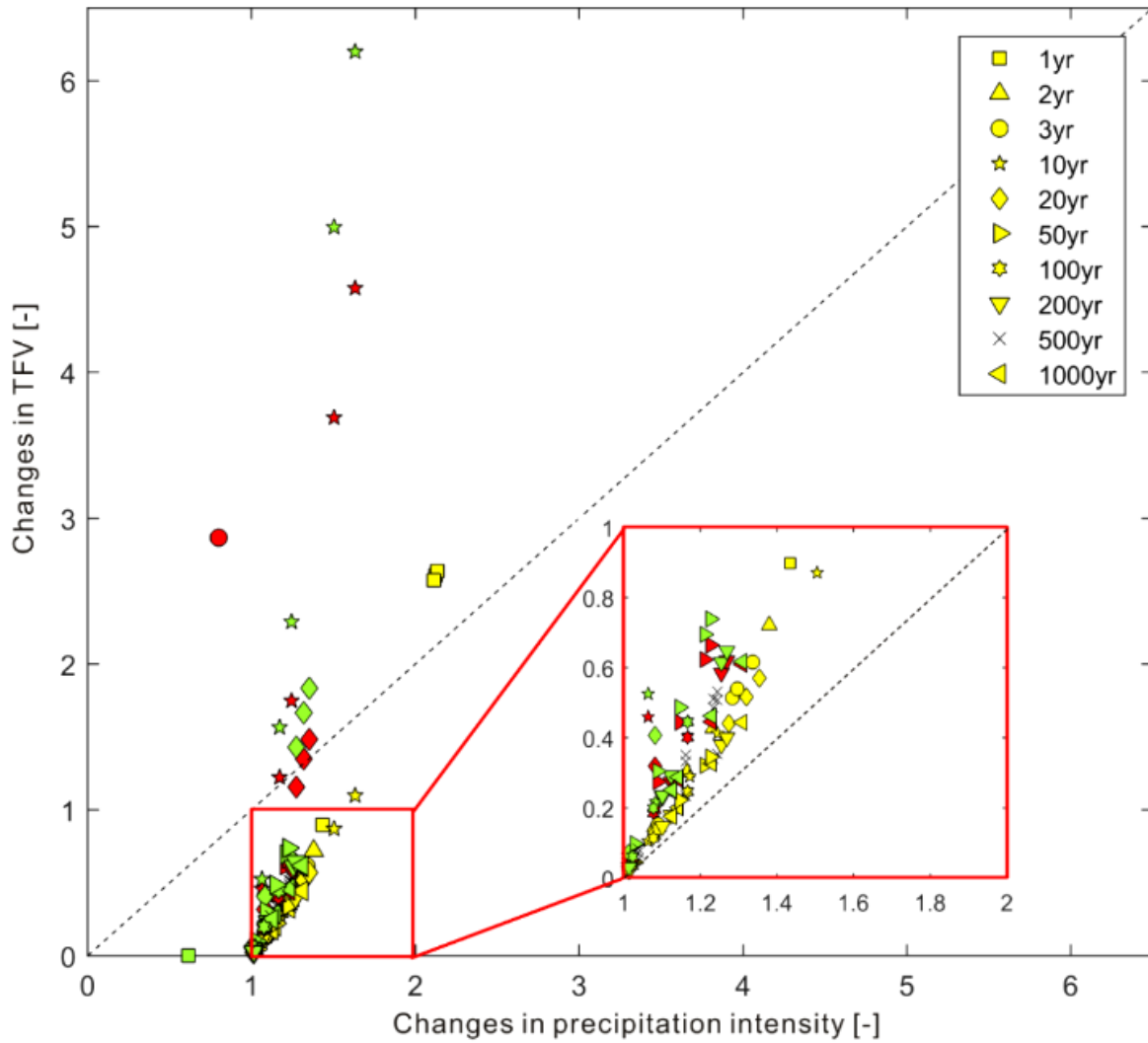
757



759

760 **Figure 5** Spatial distribution of overloaded pipelines (red colour) induced by the 3-year (left
 761 column) and 50-year extreme events (right column) without and with adaptations. The total
 762 percentage of overloaded manholes (POM) and ratio of flood volume (RFV) to input rainfall
 763 volume are summarised for each scenario. Historical flood points and local land use, mainly the
 764 traffic network and green spaces, are shown in (a).

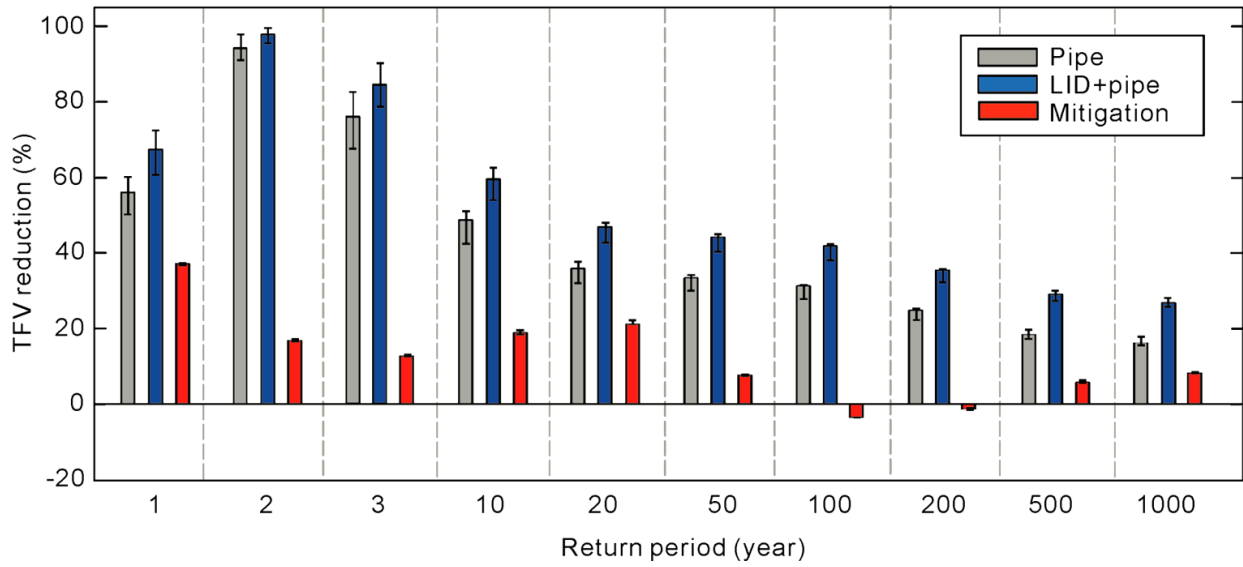
765



766

767 **Figure 6** Future changes in flood volumes (CTFVs) relative to historical conditions under the
 768 current drainage system (yellow) and two adaptation scenarios (i.e., Pipe in red and Pipe+LID in
 769 green) at various return periods.

770



771

772 **Figure 7** Comparison of benefits of climate mitigation and two adaptation strategies in reducing
 773 urban flood volumes with changes in precipitation intensities for various return periods, and with
 774 related variations (boundary bars) as a result of uncertainty arising from local soil conditions.